Physical Ergonomics and Human Factors, Vol. 63, 2022, 187–195
https://doi.org/10.54941/ahfe1002612

Plantar Soft Tissue Stiffness Automatic Estimation in Ultrasound Imaging on Deep Learning

Yori Pusparani[1,2], Ben-Yi Liau[3], Yih-Kuen Jan[4,5,6], Hsu-Tang Cheng[7], Peter Ardhianto[1,8], Fityanul Akhyar[9,10], Chi-Wen Lung[4,11*], and Chih-Yang Lin[9]**

[1]Department of Digital Media Design, Asia University, Taichung 41354, Taiwan
[2]Visual Communication Design Study Program, Budi Luhur University, Jakarta 12260, Indonesia
[3]Department of Biomedical Engineering, Hungkuang University, Taichung 413305, Taiwan
[4]Rehabilitation Engineering Lab, University of Illinois at Urbana-Champaign, Champaign, IL 61820, USA
[5]Kinesiology & Community Health, University of Illinois at Urbana-Champaign, Champaign, IL 61820, USA
[6]Computational Science & Engineering, University of Illinois at Urbana-Champaign, Champaign, IL 61820, USA
[7]Division of Plastic and Reconstructive Surgery, Department of Surgery, Asia University Hospital, Taichung 41354, Taiwan
[8]Department of Visual Communication Design, Soegijapranata Catholic University, Semarang 50234, Indonesia
[9]Department of Electrical Engineering, Yuan Ze University, Chung-Li 32003, Taiwan
[10]School of Electrical Engineering, Telkom University, Bandung – West Java 40257, Indonesia
[11]Department of Creative Product Design, Asia University, Taichung 41354, Taiwan

ABSTRACT

Preventing diabetic foot ulcers (DFU) is critical for diabetes mellitus (DM) patients. Increased stiffness of plantar foot may cause higher plantar pressure leading to a higher risk of DFU. Soft tissue stiffness can be determined by measuring the soft tissue thickness with indentation depth and stress. Therefore, we hypothesized that the deep learning model could detect the ultrasound image pixel change under soft tissue compression. This study aimed to apply the deep learning model to analyze the ultrasound image pixel thickness of plantar foot, then predict the soft tissue indentation depth and loading force for estimating the stiffness. This study has developed a motor-driven ultrasound indentation system to apply programmable compression and simultaneously assess soft tissue mechanical properties and responses in indentation depth and loading force. In addition, the effective Young's modulus was calculated to characterize mechanical properties of soft tissues in the first metatarsal head. The deep learning method employed the YOLOv5x model to train and detect the small object in the indentation depth, such as ultrasound image pixel changes. Finally, the dataset images were processed with labeling annotation from the soft tissue indentation depth and loading force. The deep learning results showed 0.995 in mean Average Precision (mAP), 0.999 in precision, 1.000 in Recall, and 0.013 in Loss. A significant correlation was found between the ultrasound image pixel changes and soft tissue indentation depth ($r = 0.98$, $p < 0.05$). Furthermore, a significant correlation was observed between the ultrasound image pixel changes and the loading force in the first metatarsal head ($r = 0.85$, $p < 0.05$). The validation and prediction models were lower than the training models in the effective Young's modulus results. However, the results of the initial modulus were similar between the three models. Our findings recommend that applying deep learning in the ultrasound image can predict soft tissue indentation depth and loading force to calculate the stiffness of the plantar foot.

Keywords: Diabetes, Diabetic foot ulcers, Effective young's modulus, Stiffness

INTRODUCTION

One of the most severe diabetes mellitus (DM) issues is diabetic foot ulcers (DFU). (Zhang et al., 2017). For people with DM, the prevention of DFU is a critical issue. The lower stiffness and higher plantar soft tissue thickness in the metatarsal head have an increased risk of DFU (Naemi et al., 2017). Furthermore, the index for evaluating soft tissue relates to indentation depth and pressure loading force (Li et al., 2006). Therefore, soft tissue stiffness can be determined by measuring the soft tissue indentation depth and pressure loading force (Makhsous et al., 2008). Ultrasound has become one of the most regularly used imaging modalities in clinical practice (Liu et al., 2019). Jan et al. also used an ultrasound indentation system to measure pressure loading force and indentation depth in plantar soft tissues (Jan et al., 2012). In addition, previous studies detect and locate the myocardial wall based on ultrasound images using a deep learning model with an accuracy of 0.900 (Zhuang et al., 2020). Thus, real-time deep learning can assist the measurement of soft tissue thickness based on B-mode ultrasound images (Ardhianto et al., 2021). Therefore, we hypothesized that the deep learning model could detect the ultrasound image pixel change under soft tissue compression. This study aimed to apply the deep learning model to detect the ultrasound image soft tissue pixel thickness, then predict soft tissue indentation depth and pressure loading force for calculating the stiffness. Understanding soft tissue stiffness may be beneficial for preventing the risk of DFU.

MATERIAL AND METHODS

This study is a pilot study, and we choose one healthy subject as a sample. The subject was a 28-years-old female with a body mass index of 17.7 kg/m^2. Our previous studies conducted the examination (Shen et al., 2021, Liau et al., 2018, Lung et al., 2016). The room temperature was maintained at 24 $\pm$ 2°C. Subject lying in supine position with an ultrasound probe position under the first metatarsal head (Figure 1A). The ultrasound images represent soft tissue under the first metatarsal head because DFU frequently occurs at pressure-sensitive sites (Perry et al., 1995).

This study has developed a motor-driven ultrasound indentation system to apply programmable compression and simultaneously assess soft tissue mechanical properties and responses in indentation depth and pressure loading force. We used the motor-driven ultrasound indentation system for the indentation tests. The motor-driven ultrasound indentation system mainly consists of four parts: stepper motor, load cell, ultrasound system, and standoff holder. In detail, a linear ultrasound probe set to 12 MHz to analyze soft tissue (5-12 MHz, 128 elements, 39 mm Array footprint, Telemed, Vilnius, Lithuania) attached to a PC-based ultrasound system (sampling rate 1000 Hz, ArtUs EXT-1H scanner, Telemed, Vilnius, Lithuania). The ultrasound probe was mounted on the stepper motor (Model TL-SL1010-X, Tanlian Electro Optics Co., Ltd., Taoyuan, Taiwan), and 49-N load cell (sampling rate 100 Hz, Model UKA-E-005, Li-Chen Measure Co., Ltd., Kaohsiung, Taiwan) (Figure 1B). Soft tissue thickness was measured using ultrasound images in

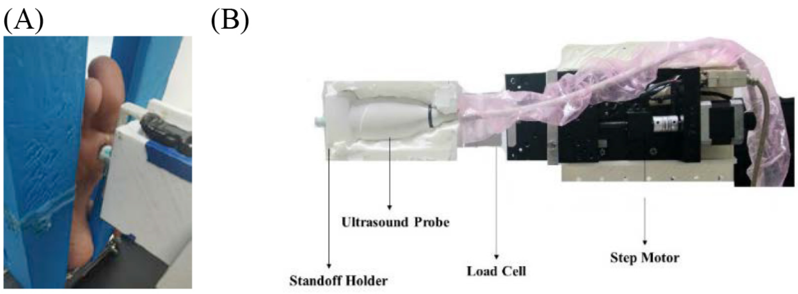

Figure 1: Soft tissue indentation measurements. (A) Ultrasound probe position in the first metatarsal head. (B) Ultrasound indentation system.

soft tissue strain ratio. Soft tissue has loading and unloading in each cycle. Therefore, indentation depth and pressure loading force are obtained simultaneously in five cycles. Additionally, we divided into two cycles become 12 sections. The 6 sections for the train data of deep learning, and another 6 sections for validation.

YOLO is a real-time object detection model that reformulates the object into a single regression issue (Redmon et al., 2016). Furthermore, YOLO employs a single neural network architecture to predict bounding boxes from dataset ultrasound images and provide faster detection (Goyal et al., 2018). Therefore, YOLO detects faster, especially for medical images (Ardhianto et al., 2021). This study built the detection with PyTorch 1.7.0 and YOLOv5x on Windows 10. The model parameters were: the batch size was 8, the momentum and weight decay rates were 0.937 and 0.0005, respectively, the learning rate was 0.01, and the epoch was 100. The tests were performed on a machine with the following specifications: Core I7 10700 CPU, 32 GB RAM, and an NVIDIA RTX 3080 10GB graphics card.

This study used 360 raw ultrasound images from 6 sections dataset containing various indentation depth. The selected images in 781 × 1563 pixels. We use the roboflow labeling platform to annotate the object and category with annotating name "thickness." The labeled pictures are divided into the training and validation sets; we used 50% (180 images) from 3 sections for training and 50% (180 images) for validation. The training section labeled the soft tissue thickness between skin and bone using the 360 bounding box in the dataset. Furthermore, we input datasets labeled to YOLOv5x models to predict soft tissue thickness.

Classifier modification for the ultrasound dataset has one object category, namely thickness. The dimension of the output tensor is $3 \times (5 + 1) = 18$, where 3 represents the three template boxes for each grid prediction, and 5 illustrates each prediction box coordinates (x, y, w, h) and confidence (confidence, c). Each anchor box is calculated with confidence values of different classes and four coordinate values (x, y, w, h), which can predict the thickness location. The prediction result of each image must be converted into an annotation with the format x_1, y_1, x_2, y_2 to calculate the original coordinates.

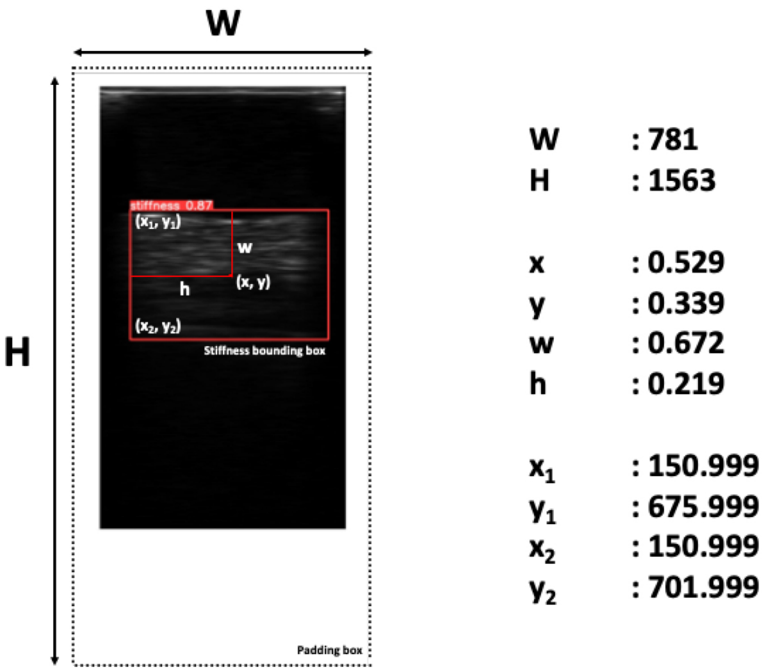

Figure 2: The example of converting YOLOv5x coordinates into pixel coordinates. YOLOv5x coordinates are ***x***, ***y***, ***w***, ***h***, ***W***, and ***H***. Pixel coordinates x_1, y_1, x_2, y_2; ***x*** and ***y***, coordinates were presenting the center of the box; ***w***, the width of the bounding box; ***h***, the height of the bounding box; ***W***, the width of the image; ***H***, the height of the image.

The YOLOv5x records four 180 corner coordinates of the bounding box prediction by converting the YOLOv5x coordinates as equation (1):

$$x_1 = \frac{y-w}{2}W), y_1 = \frac{x-w}{2}W, x_2 = \frac{y-w}{2}W, y_2 = \frac{x+w}{2}W \quad (1)$$

Where x_1, y_1 represents the bounding box coordinates of soft tissue thickness and x_2, y_2 represents the bottom of the bounding box coordinates (Figure 2). The center of the soft tissue thickness bounding box is x and y, the width and height of the bounding box area are w and h, and the width and height of the images are W and H. In detail, x_1 and y_1 are the top-left corner coordinates, and the below-left corner soft tissue thickness bounding box is x_2 and y_2.

The distance between skin and bone was measured using the distance formula. After getting the distance result, we calculated the section average of 180 steps in 12 sections, loading and unloading into 6 sections. Equation (2) shows the distance formula:

$$d = \sqrt{(x_2 - x_1)^2 + (y_2 - y_1)^2} \quad (2)$$

where d is the symbol of distance to calculate the distance between the skin and bone of soft tissue for measurements.

Regression analysis was performed to determine the correlation between soft tissue thickness pixel, indentation depth, and pressure loading force. The effective Young's modulus (E) is a traditional material constant to quantify elastic properties of soft tissues (Hayes et al., 1972, Zheng and Mak, 1999). The equation used to extract effective Young's modulus E is defined as equation (3):

$$E = \frac{(1 - v^2)}{2a \bullet k(v, a/h)} \bullet \frac{P}{w} \tag{3}$$

where $\boldsymbol{v}$ is the Poisson's ratio, $\boldsymbol{a}$ is the indenter radius, $\boldsymbol{k}$ is a scaling factor dependent on the Poisson's ratio, indenter radius, and tissue thickness, $\boldsymbol{h}$ is the soft tissue thickness, $\boldsymbol{P}$ is the loading force, and $\boldsymbol{w}$ is the indentation depth. Generally, 0.45 has been used as the Poisson's ratio for biological soft tissues (Zheng and Mak, 1999). The $\boldsymbol{k}$ value was obtained from the information extracted from the publication of Hayes and colleagues (Hayes et al., 1972).

The correlations between soft tissue indentation depth of YOLOv5x prediction and soft tissue indentation depth and soft tissue pressure loading force were determined using a Pearson product-moment correlation analysis. All statistical tests were performed using SPSS 25 (IBM, NY, USA) at the significance level of 0.05.

RESULT

The accuracy of bounding box detecting ultrasound images in soft tissue thickness was shown 0.995 in mean Average Precision (mAP), 0.999 in precision, 1.000 in Recall, and 0.013 in Loss. The accuracy has become the most popular metric to evaluate object detection models (Nasirahmadi et al., 2019). A high mAP means that the trained model performs well (Kumar and Punitha, 2020). Significant correlations between the soft tissue image pixel thickness and indentation depth ($r = 0.98, p < 0.05$) and the soft tissue image pixel thickness and pressure loading force ($r = 0.85$, $p < 0.05$) in the first metatarsal head as shown in Figure 3. The percentage of effective Young's modulus (*E1*, *E2*, and *E3*) was 1%, 4%, and 14% between the validation model and prediction model (Figure 4).

DISCUSSION

This study demonstrated that the YOLOv5x model detected soft tissue thickness to predict the indentation depth and pressure loading force under the first metatarsal head. Therefore, we hypothesized that YOLOv5x could detect soft tissue thickness, consistent with the hypothesis of this study. The accuracy of the YOLOv5x model is based on our prediction using the bounding box. Besides that, we also have significant correlations between the thickness detection of YOLOv5x with soft tissue loading indentation depth and pressure loading force. The r-value has shown a good result.

This study was compared with other studies to measure thickness using deep learning. However, other studies use different methods, such as

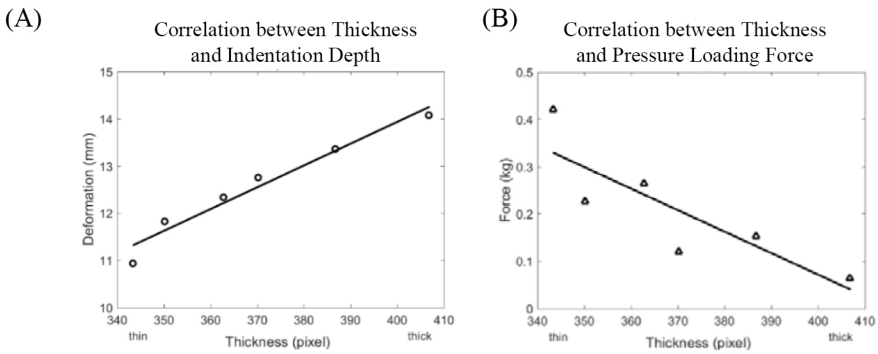

Figure 3: The scatter plots show the relationship between the image pixel thickness detection of Yolo with soft tissue loading property changes. (A) Correlation between pixel thickness and the indentation depth. (B) Correlation between pixel thickness and pressure loading force. (*, $p < 0.05$; **, $p < 0.01$).

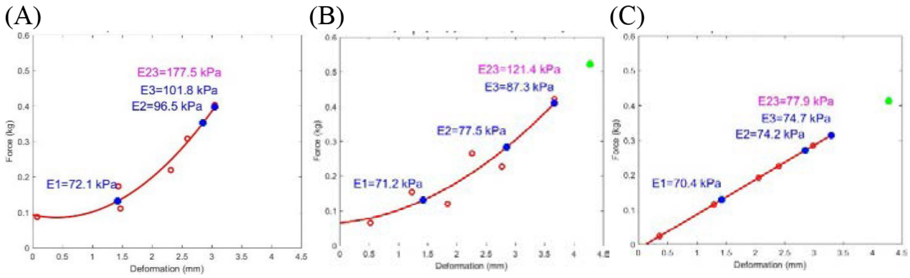

Figure 4: The effective Young's modulus. (A) Training data. (B) Validation data. (C) Regression prediction data. (***E1***, Initial modulus; ***E2***, nonlinear modulus; ***E3***, effective Young's modulus).

Table 1. The comparison of detection performance with the related literature study.

References	Study Case	Method	Accuracy
Yen et al. 2008	Tissue Thickness	ANN	0.920
Foersch et al. 2021	Soft Tissue Sarcoma	DenseNet121	0.871
This study	Soft Tissue Thickness	YOLOv5x	0.995

Note: **ANN**, Artificial Neural Network; **DenseNet121**, Densely Connected Convolutional Network; **YOLO**, You Only Look Once.

Yen et al. using the ANN model to predict tissue thickness has 0.920 accuracies (Yen et al., 2008). Foersch et al. used the DenseNet12 model to predict soft tissue sarcoma with 0.871 accuracies (Foersch et al., 2021). According to the results of Guo et al., ultrasound images with YOLO have better accuracy (Guo et al., 2021). The detection performance comparison with the related literature study is in Table 1.

A model for soft tissues to be represented in the hysteresis loop of dynamic systems in loading and unloading conditions (Safadi and Rubin, 2014). We choose the middle in two cycles; one section is for the training, another section is for validation. The value can be presented as improving indentation depth and pressure loading force of soft tissue. As proposed by Fung et al., a commonly used model to characterize hysteresis loops of tissue can be modeled by characterizing the loading curve and the unloading curve (Fung, 1993). Soft tissue exhibits hysteresis in a loading-unloading test. Hence, we used hysteresis to predict soft tissue indentation depth and pressure loading force. Therefore, for training validation were used polynomial to get the value of soft tissue thickness correlation with indentation depth and pressure loading force (Brody et al., 1981).

In this study, we have two limitations. First, we use the deep learning model to train and detect the thickness using the bounding box. This paper only uses one box for each image to measure the image pixel thickness. In contrast, machine learning refers to Scikit learning that may be more efficient and fast to get the regression result (Raschka and Mirjalili, 2019). Future studies may consider applying machine learning to get the regression result directly. Second, the limitation in this study used combined data between loading and unloading to predict soft tissue thickness. Predicting the soft tissue thickness separately during loading and unloading would provide a more detailed measurement of soft tissue stiffness change in future studies.

CONCLUSION

A significant correlation was found between the ultrasound image pixel changes and the soft tissue indentation depth. Furthermore, a significant correlation was also getting between the ultrasound image pixel changes and the soft tissue pressure loading force in the first metatarsal head. The validation and prediction models were lower than the training models in the effective Young's modulus results. However, the results of the initial modulus are similar between the three models. Our findings suggest that applying deep learning in the ultrasound image can be predicted soft tissue indentation depth and pressure loading force to calculate the initial stiffness.

ACKNOWLEDGMENT

The authors wish to express gratitude to Mr. Fahni Haris, Mr. Wei-Cheng Shen, and Mr. Jifeng Wang for their assistance. This study was supported by a grant from the Ministry of Science and Technology of the Republic of China (MOST 110-2221-E-468-005 and MOST 110-2221-E-155-039-MY3). The funding agency did not have any involvement in data collection, data analysis, and data interpretation.

REFERENCES

Ardhianto, P., Tsai, J.-Y., Lin, C.-Y., Liau, B.-Y., Jan, Y.-K., Akbari, V.-B.-H. et al. (2021). "A Review of the Challenges in Deep Learning for Skeletal and Smooth Muscle Ultrasound Images". *Applied Sciences,* Vol. 11, no. 9, p. 4021.

Brody, W.R., Butt, G., Hall, A. and Macovski, A. (1981). "A method for selective tissue and bone visualization using dual energy scanned projection radiography". *Medical physics,* Vol. 8, no. 3, pp. 353-57.

Foersch, S., Eckstein, M., Wagner, D.-C., Gach, F., Woerl, A.-C., Geiger, J. et al. (2021). "Deep learning for diagnosis and survival prediction in soft tissue sarcoma". *Annals of Oncology,* Vol. 32, no. 9, pp. 1178–87.

Fung, Y.-C. (1993). Mechanical properties and active remodeling of blood vessels. *Biomechanics*. Springer.

Goyal, M., Reeves, N.D., Davison, A.K., Rajbhandari, S., Spragg, J. and Yap, M.H. (2018). "Dfunet: Convolutional neural networks for diabetic foot ulcer classification". *IEEE Transactions on Emerging Topics in Computational Intelligence,* Vol. 4, no. 5, pp. 728–39.

Guo, D., Zhang, G., Peng, H., Yuan, J., Paul, P., Fu, K. et al. (2021). "Segmentation and Measurements of Carotid Intima-Media Thickness in Ultrasound Images Using the Improved Convolutional Neural Network and Support Vector Machine". *Journal of Medical Imaging and Health Informatics,* Vol. 11, no. 1, pp. 15–24.

Hayes, W.C., Keer, L.M., Herrmann, G. and Mockros, L.F. (1972). "A mathematical analysis for indentation tests of articular cartilage". *Journal of Biomechanics,* Vol. 5, no. 5, pp. 541–51.

Jan, Y.-K., Lung, C.-W., Cuaderes, E., Rong, D. and Boyce, K. (2012). "Effect of viscoelastic properties of plantar soft tissues on plantar pressures at the first metatarsal head in diabetics with peripheral neuropathy". *Physiological Measurement,* Vol. 34, no. 1, p. 53.

Kumar, C. and Punitha, R. "Yolov3 and yolov4: Multiple object detection for surveillance applications". 2020 Third International Conference on Smart Systems and Inventive Technology (ICSSIT)2020, IEEE.

Li, X., Wang, G., Huang, L. and Zhang, G. (2006). "Young's modulus extraction methods for soft tissue from ultrasound measurement system". *Instrumentation Science and Technology,* Vol. 34, no. 4, pp. 393-404.

Liau, B.-Y., Chen, C.-L., Jan, Y.-K., Chiu, H.-Y., He, P.-S. and Lung, C.-W. "A comparative study of the effects of electrical stimulation and intermittent compressive forces on soft tissue mechanical properties". AHFE 2017 International Conference on Physical Ergonomics and Human Factors, 2017, July 17, 2017 - July 21, 20172018, *Los Angeles, CA, United states*. Springer Verlag.

Liu, S., Wang, Y., Yang, X., Lei, B., Liu, L., Li, S.X. et al. (2019). "Deep Learning in Medical Ultrasound Analysis: A Review". *Engineering,* Vol. 5, no. 2, pp. 261–75.

Lung, C.W., Cheng, T.Y., Li, Y.J., Liau, B.Y. and Jan, Y.K. (2016). "Development of an intermittent pneumatic compression system to manage soft tissue mechanical properties". *Advances in Intelligent Systems and Computing,* Vol. 482, pp. 317–25.

Makhsous, M., Venkatasubramanian, G., Chawla, A., Pathak, Y., Priebe, M., Rymer, W.Z. et al. (2008). "Investigation of soft-tissue stiffness alteration in denervated human tissue using an ultrasound indentation system". *The journal of spinal cord medicine,* Vol. 31, no. 1, pp. 88–96.

Naemi, R., Chatzistergos, P., Suresh, S., Sundar, L., Chockalingam, N. and Ramachandran, A. (2017). "Can plantar soft tissue mechanics enhance prognosis of diabetic foot ulcer?". *Diabetes research and clinical practice,* Vol. 126, pp. 182–91.

Nasirahmadi, A., Sturm, B., Edwards, S., Jeppsson, K.-H., Olsson, A.-C., Müller, S. et al. (2019). "Deep learning and machine vision approaches for posture detection of individual pigs". *Sensors,* Vol. 19, no. 17, p. 3738.

Perry, J.E., Ulbrecht, J.S., Derr, J.A. and Cavanagh, P.R. (1995). "The use of running shoes to reduce plantar pressures in patients who have diabetes". *The Journal of bone and joint surgery. American volume,* Vol. 77, no. 12, pp. 1819–28.

Raschka, S. and Mirjalili, V. (2019). *Python machine learning: Machine learning and deep learning with Python, scikit-learn, and TensorFlow 2*. Packt Publishing Ltd.

Redmon, J., Divvala, S., Girshick, R. and Farhadi, A. "You only look once: Unified, real-time object detection". Proceedings of the IEEE conference on computer vision and pattern recognition2016.

Safadi, M. and Rubin, M. (2014). "Modeling rate-independent hysteresis in large deformations of preconditioned soft tissues". *International Journal of Solids and Structures,* Vol. 51, no. 18, pp. 3265–72.

Shen, W.-C., Jan, Y.-K., Lung, C.-W., Chen, H.-C., Li, C.-T., Bau, J.-G. et al. "Using Ultrasound to Assess Microchambers and Macrochambers Tissue Properties After Walking at Different Speeds and Durations". 2021, *Cham*. Springer International Publishing.

Yen, P.-L., Chen, D.-R., Yeh, K.-T. and Chu, P.-Y. (2008). "Lateral exploration strategy for differentiating the stiffness ratio of an inclusion in soft tissue". *Medical engineering & physics,* Vol. 30, no. 8, pp. 1013–19.

Zhang, P., Lu, J., Jing, Y., Tang, S., Zhu, D. and Bi, Y. (2017). "Global epidemiology of diabetic foot ulceration: a systematic review and meta-analysis". *Annals of medicine,* Vol. 49, no. 2, pp. 106-16.

Zheng, Y. and Mak, A.F. (1999). "Effective elastic properties for lower limb soft tissues from manual indentation experiment". *IEEE Transactions on Rehabilitation Engineering,* Vol. 7, no. 3, pp. 257–67.

Zhuang, Z., Liu, G., Ding, W., Raj, A.N.J., Qiu, S., Guo, J. et al. (2020). "Cardiac VFM visualization and analysis based on YOLO deep learning model and modified 2D continuity equation". *Computerized Medical Imaging and Graphics,* Vol. 82, p. 101732.